Available online at www.sciencedirect.com

ScienceDirect

journal homepage: www.elsevier.com/locate/he

Closed loop torque SVM-DTC based on robust super twisting speed controller for induction motor drive with efficiency optimization

Abdelkarim Ammar[*], *Abdelhamid Benakcha*, *Amor Bourek*

Electrical Engineering Laboratory of Biskra LGEB, University of Biskra, Biskra BP 145, Algeria

ARTICLE INFO

Article history:
Received 13 November 2016
Received in revised form
25 March 2017
Accepted 6 April 2017
Available online xxx

Keywords:
Induction motor
Direct torque control (DTC)
Efficiency optimization
Loss model control (LMC)
Super twisting
dS1104

ABSTRACT

This paper presents a space vector modulation (SVM) based Direct Torque Control strategy (DTC) for induction motor (IM) in order to overcome the drawbacks of the classical DTC. SVM can reduce the high torque and flux ripples by preserving a fixed switching frequency. This technique is known by the closed loop torque SVM-DTC. Moreover, the control scheme performance is improved by inserting a second order sliding mode super twisting controller in the outer loop for speed regulation. This nonlinear technique ensures a good dynamic and high robustness against external disturbance. Furthermore, the IM energy optimization is treated in the second objective of this paper. A proposed model based loss minimization strategy is presented for efficiency optimization. This strategy chooses an optimal flux magnitude for each applied load torque. The proposed optimized SVM-DTC algorithm will be investigated by simulation and real time implementation using Matlab/Simulink with real time interface based on dSpace 1104 signal card.

Introduction

The Direct Torque Control (DTC) strategy is known by its simple decoupled scheme for stator flux and electromagnetic torque control. Unlike the field oriented control (FOC), DTC has more advantages like fast response and less dependence to machine's parameters. Moreover, it doesn't require coordinate transformation or current regulation loops. It bases on the selecting of an appropriate voltage vectors for the inverter which fed the motor through hysteresis controllers and look-up switching table. However, due to its structure, the main problems of this method are the high level of torque and flux ripples and the variable switching frequency, they cause by consequence an acoustical noise and increase control difficulty at low speed regions [1,2].

Recently, different methods were proposed to overcome these drawbacks. The multilevel converters can provide low ripples [3]. Nevertheless, they increase the number of power switches which lead to a high cost and reduce the efficiency of the control system. The intelligent techniques like fuzzy logic and artificial neural networks have been investigated in many researches. However, they are usually very complex and require powerful calculation processes. The model predictive control (MPC) also has the ability to determine a suitable voltage vectors choice which can reduce the ripples [4]. However, the high complexity of the control law makes the main disadvantage to realize this strategy. The constant

* *Corresponding author.*
E-mail address: ammar.abdelkarim@yahoo.fr (A. Ammar).
http://dx.doi.org/10.1016/j.ijhydene.2017.04.034

Nomenclature

DTC	Direct Torque Control
SVM	Space Vector Modulation
$i_{s\alpha}$ $i_{s\beta}$	α and β components of stator currents
$V_{s\alpha}$ $V_{s\beta}$	α and β components of stator voltage
$\psi_{s\alpha}$ $\psi_{s\beta}$	α and β components of stator flux
R_s R_r	Stator and rotor resistances
L_s L_r	Stator and rotor inductances
σ	Blondel's coefficient
Msr	Stator–rotor mutual inductance
T_e	Electromagnetic torque
ψ_s	Stator flux magnitude
p	Number of poles pairs
DSP	Digital signal processor
T_1 T_2	Reference voltages vectors corresponding durations
T_z	Sampling time
V_{dc}	DC bus voltage
ω	Rotor speed
J	Inertia moment
f	Coefficient of friction
T_L	Load torque
VSI	Voltage Source Inverter
SFOC	Stator Field Oriented Control
THD	Total harmonics distortion
RTI	Real Time interface
SMC	Sliding mode control
STSC	Super twisting speed controller
LMC	Loss model control

switching frequency DTC methods using the space vector modulation (SVM) have been proposed as well to face those problems. The SVM direct torque control replaces the switching table by voltage modulator for the calculation of the switching states for the voltage source inverter (VSI). The aim of SVM is to select an appropriate switching vectors in order to minimize current harmonic distortion and torque/flux ripples by maintaining the switching frequency constant. Moreover, SVM-DTC structure is independent on IM rotor parameters. Different SVM-DTC structures have been proposed in literature. The stator flux oriented control (SFOC-DTC) with SVM and the load angle based closed loop torque control are widely discussed [2,5,6]. The closed loop torque control become our interest in this paper. This control scheme keeps the simplicity of the basic DTC, where it is designed in the stationary reference frame. It bases on the changes in motor's torque to achieve an appropriate voltage vector [5,7].

Furthermore, the DTC strategy can be enhanced by inserting robust controllers to improve the stability and the robustness of the entire control scheme. Different, nonlinear control techniques have been proposed for induction motor to improve control's performances like fast dynamic response, good support for external load disturbance and rejection capabilities [8,9]. The sliding mode control (SMC) method offers an excellent dynamic and high robustness of the IM drive. In addition, it has a simple software and hardware implementation. The higher order sliding mode control is presented in order to eliminate the chattering phenomenon which is the main problem of the conventional SMC (i.e. first order SMC) [9]. For this, the super twisting is a second order sliding mode technique which is proposed to provide a continuous control in order to reduce the effect of chattering while keeping the desirable properties of the first order SMC (i.e., fast response and high robustness) [10,11]. Recently, this strategy have acquired a big attention in serval control applications, in Ref. [12] a comparative study between different second order SMC strategies are implemented for wind energy conversion system to optimize its power efficiency. Then, in Refs. [13,14] the super twisting technique have shown high performance in fuel cell's system control. For the same purpose, this paper presents a super twisting control design for the outer speed regulation loop to improve the robustness and the stability of the control algorithm.

Although the advantages of the proposed control strategy, it can get more high performance by achieving the maximum of efficiency. Another objective of this paper, is that the DTC control scheme will be associated to an efficiency maximization strategy based on losses minimization. This strategy is related to the choice of the proposed flux level according to the desired load value. It is known that the high flux values increase the iron losses in magnetic circuit while the low values increase the copper losses. Thus, an optimal flux value should be chosen [15]. Several researchers have proposed concerning the choice of the optimal flux reference. The well-known efficiency improvement strategies are divided into two categories, search controller (SC) and loss-model-based control (LMC) [16]. The main drawbacks of the search control are the slow convergence and torque ripples [17]. The model based optimization method which called loss model control (LMC) has been described in Ref. [16]. It uses the steady-state IM model in the rotor flux field orientation coordinate frame to generate the optimal flux reference which will be tuned online and make the machine efficiency optimized. This optimization has been applied for DTC control scheme in several works [15,18].

This paper aims to present a closed loop torque control SVM-DTC with model based loss minimization strategy for the purpose of efficiency optimization. In addition, a robust super twisting speed controller (STSC) will be inserted to improve comprehensively the control scheme performance by providing fast speed response and high robustness against external load disturbance. The results will be examined by simulation using Matlab/Simulink software. Moreover, an experimental validation will be presented also by the real-time interface (RTI) linked with dSpace 1104 board.

This paper is organized as follows: Section Closed loop torque DTC strategy using SVM presents the closed loop torque strategy with SVM. Section Efficiency optimization strategy: loss model control presents the model based efficiency optimization strategy. Then, in Section Robust speed regulation, the robust speed control design is presented. Section Stator flux estimation presents a simple modified flux estimation technique. Section Simulation and experimental results presents the control strategy investigation by simulation and hardware implementation.

Please cite this article in press as: Ammar A, et al., Closed loop torque SVM-DTC based on robust super twisting speed controller for induction motor drive with efficiency optimization, International Journal of Hydrogen Energy (2017), http://dx.doi.org/10.1016/j.ijhydene.2017.04.034

Closed loop torque DTC strategy using SVM

The main difference between the classical and the SVM based DTC strategies, is that SVM-DTC have replaced the switching table by SVM unit for the switching signals calculation [7]. The optimal selection of the space voltage vectors in each sampling period preserves a constant switching frequency which reduce considerably torque/flux ripples. Consequently, the SVM-DTC can achieve an effective control of the stator flux and torque.

The closed loop torque control using SVM which so called also the load angle control become our interest in this paper. This method bases on the adjustment of the motor's torque changes using only one PI controller in order to produce an appropriate voltage vector [19]. Furthermore, the design of this strategy is done in the stationary frame without requesting coordinate transformation unlike the SFOC-DTC.

Induction motor model

The dynamic equation's model of the induction motor can be written in the stationary reference frame with assuming the stator current and the stator flux as state variables. It is expressed in Eq. (1) by:

$$\begin{cases} \dfrac{di_{s\alpha}}{dt} = -\left(\dfrac{R_s}{\sigma L_s} + \dfrac{R_r}{\sigma L_r}\right) i_{s\alpha} - \omega_r i_{s\beta} + \dfrac{R_s}{\sigma L_s L_r}\psi_{s\alpha} + \dfrac{\omega_r}{\sigma L_r}\psi_{s\beta} + \dfrac{1}{\sigma L_s}u_{s\alpha} \\ \dfrac{di_{s\beta}}{dt} = -\left(\dfrac{R_s}{\sigma L_s} + \dfrac{R_r}{\sigma L_r}\right) i_{s\beta} + \omega_r i_{s\alpha} + \dfrac{R_s}{\sigma L_s L_r}\psi_{s\beta} - \dfrac{\omega_r}{\sigma L_r}\psi_{s\alpha} + \dfrac{1}{\sigma L_s}u_{s\beta} \\ \dfrac{d\psi_{s\alpha}}{dt} = u_{s\alpha} - R_s i_{s\alpha} \\ \dfrac{d\psi_{s\beta}}{dt} = u_{s\beta} - R_s i_{s\beta} \end{cases} \quad (1)$$

where:

$i_{s\alpha}$, $i_{s\beta}$ are stator current components. $\psi_{s\alpha}$, $\psi_{s\beta}$ are stator flux components.
R_s, R_r are stator and rotor resistances. L_s, L_r are stator and rotor inductances.
$\sigma = 1 - \frac{M_{sr}}{L_s L_r}$ is Blondel's coefficient. M_{sr} is the mutual stator-rotor inductance.

The electromagnetic torque can be expressed by:

$$T_e = p(\psi_{s\alpha} i_{s\beta} - \psi_{s\beta} i_{s\alpha}) \quad (2)$$

p is the number of pole pairs.

Load angle control

In this control scheme, the torque of the motor can be adjusted by the change of the angle δ between the stator and the rotor flux vectors which is called the load angle (Fig. 1).

The torque of induction motor can be expressed in terms of stator and rotor flux vectors as follow:

$$T_e = p\frac{M_{sr}}{\sigma L_s L_r}\psi_s \times \psi_r = p\frac{M_{sr}}{\sigma L_s L_r}|\psi_s||\psi_r|\sin(\delta) \quad (3)$$

The main objective of this strategy is to select a reference voltage vector V_s^* which changes ψ_s, then modulate it by SVM technique. The produced change of the load angle which produced by the PI torque controller in added to the actual angle of the rotor flux vector. Therefore, the reference stator flux vector can be computed by the following formula Eq. (4), it is expressed as a polar-to rectangular transformation [5,7,19].

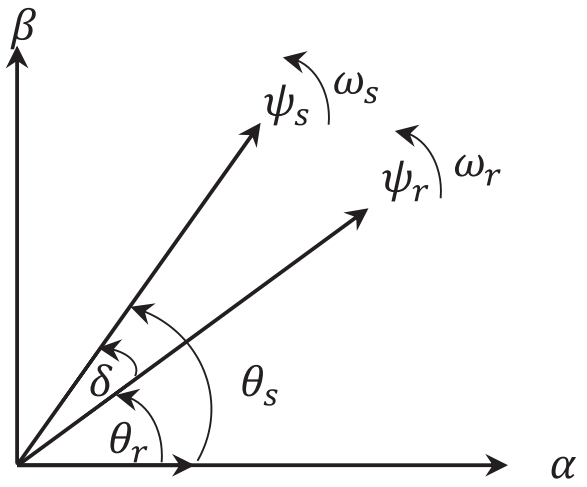

Fig. 1 – Stator and rotor flux vectors and angles.

$$\psi_s^* = |\psi_s^*|\cos(\delta + \theta_r) + j|\psi_s^*|\sin(\delta + \theta_r) \quad (4)$$

θ_r is the rotor flux angle.

To generate the required torque, the stator reference voltages ($V_{s\alpha}^*$,$V_{s\beta}^*$) are responsible of changing the rotating velocity of stator flux vector while keeping its amplitude constant. They can be calculated based on the stator flux error and sampling time in (α, β) frame by:

$$\begin{cases} V_{s\alpha}^* = \dfrac{\psi_{s\alpha}^* - \widehat{\psi}_{s\alpha}}{T_z} + R_s i_{s\alpha} \\ V_{s\beta}^* = \dfrac{\psi_{s\beta}^* - \widehat{\psi}_{s\beta}}{T_z} + R_s i_{s\beta} \end{cases} \quad (5)$$

T_z is the sampling time.

PI controller design

The reference torque T_e^* is produced by the speed controller. Then, it is compared with the estimated torque $\widehat{T}_e$. The obtained error signal is the input of the PI torque controller that computes the instantaneous value of slip angular frequency ω_{sl}^*. This latter is the derivative of the load angle δ which required to adjust the stator flux angle [19]. The relationship between the reference electromagnetic torque T_e^* and slip angular frequency ω_{sl}^* can be determined as following:

Eq. (3) can be written as:

$$T_e = p\frac{M_{sr}}{\sigma L_s L_r}|\psi_s|e^{j\omega_s t} \times |\psi_r|e^{j\omega_r t} = \left[p\frac{M_{sr}^2}{R_r L_s^2}|\psi_s|^2\right]\left[1 - e^{-t/T_M}\right](\omega_s - \omega_r) \quad (6)$$

where $T_M = \sigma\frac{L_r}{R_r}$.

The relationship between stator angular frequency ω_s and rotor angular frequency ω_r is slip angular frequency ω_{sl} which it is expressed by:

Please cite this article in press as: Ammar A, et al., Closed loop torque SVM-DTC based on robust super twisting speed controller for induction motor drive with efficiency optimization, International Journal of Hydrogen Energy (2017), http://dx.doi.org/10.1016/j.ijhydene.2017.04.034

$$\omega_{sl} = \omega_s - \omega_r \tag{7}$$

Then, the electromagnetic torque expression becomes:

$$T_e = \left[p\frac{M_{sr}^2}{R_r L_s^2}|\psi_s|^2\right]\left[1 - e^{-t/T_M}\right]\omega_{sl} \tag{8}$$

From Eq. (8), it is noticed that the relationship between torque and slip angular frequency is so clear. The transfer function is achieved by Laplace transform as:

$$G(s)_{T_e} = \frac{\widehat{T}_e}{\omega_{sl}^*} = \frac{K_{T_e}}{1 + T_M s} \tag{9}$$

where $K_{T_e} = p\frac{M_{sr}^2}{R_r L_s^2}|\psi_s|^2$.

The PI controller design can be given by:

$$\left[K_p s + \frac{K_i}{s}\right]\left(T_e^*(s) - \widehat{T}(s)\right) \tag{10}$$

K_p and K_i are the proportional and integral gains.

The used determination method for the controller gains is pole placement method.

The load angle δ can be determined by the integration of produced slip frequency ω_{sl}. Then, the input of the polar-to-rectangular transformation of the stator flux is the addition of the load angle with the rotor flux angle.

Space vector modulation

The torque ripples in the classical DTC are affected proportionally by the width of the hysteresis band. However, even when the bandwidth is reduced, the torque ripples are still important due to the discrete nature of the hysteresis controller. Furthermore, the very small bandwidths values increase inverter switching frequency and switching losses [20]. The use of SVM preserves a constant switching frequency, consequently, the ripples of the stator flux and torque and switching losses can be reduced.

The principle of SVM is to predict and to calculate the voltage vector. It based on each three adjacent vectors in each sector for two-level inverter. The application time for each vector can be obtained by vector calculations and the rest of the time period will be spent by applying the null vector [7]. For two-level inverter, the space vector diagram is shown in Fig. 2.

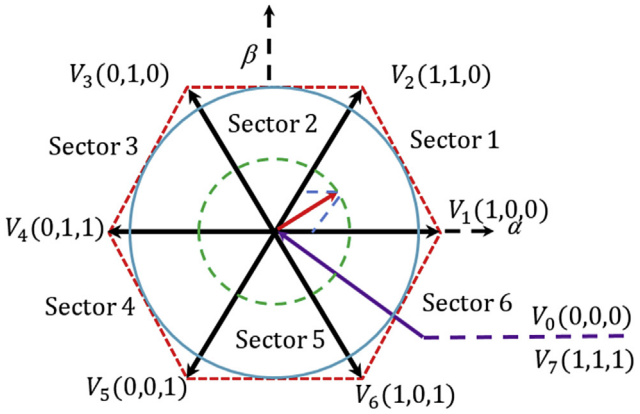

Fig. 2 – Diagram of voltage space vector for 2-level inverter.

$$T_1 = \frac{T_z}{2V_{dc}}\left(\sqrt{6}V_{s\beta}^* - \sqrt{2}V_{s\alpha}^*\right) \tag{11}$$

$$T_2 = \sqrt{2}\,\frac{T_s}{U_{dc}}V_{s\alpha}^* \tag{12}$$

T_1 and T_2 are the corresponding vector durations.
V_{dc}: DC-bus voltage.

Efficiency optimization strategy: loss model control

Loss model

Generally, the different losses of the induction machine can be classified into three categories, stator copper losses, rotor copper losses and stator core losses. The copper losses represent the ohmic losses in the stator and the rotor. The inverter losses can also be ignored for low-power IM drives [16]. By using the steady-state induction motor equivalent circuit (Fig. 3) in the synchronous reference, the motor copper losses are defined by Refs. [16,18]:

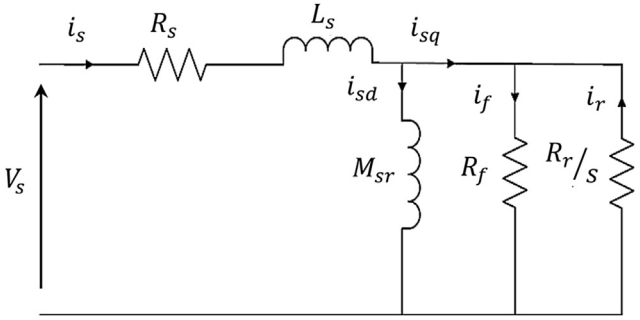

Fig. 3 – Induction motor steady-state equivalent circuit, where s is the slip and R_f is iron losses resistance.

$$\begin{cases} P_s = R_s\left(i_{sd}^2 + i_{sq}^2\right) \\ P_r = R_r\left(i_{rd}^2 + i_{rq}^2\right) = R_r\left[\left(\frac{\psi_r}{L_r} - \frac{M_{sr}}{L_r}i_{sd}\right)^2 + \left(\frac{M_{sr}}{L_r}\right)^2\right] \end{cases} \tag{13}$$

The stator core losses constituted by the hysteresis and eddy-current losses:

$$P_{fs} = P_{hs} + P_{es} = K_h f_s \psi_s^2 + K_e f_s^2 \psi_s^2 \tag{14}$$

The rotor core losses are very small compared with stator losses and they are mostly neglected.

Where:

P_s, P_r: are stator and rotor copper losses respectively, i_{sd}, i_{sq}: are direct and quadratic components of the stator current, P_{fs}: stator core losses, P_{hs}, P_{es}: stator hysteresis and eddy-current losses respectively, K_h, K_e: hysteresis and eddy-current coefficients related to the magnetic circuit properties, f_s: stator frequency.

Please cite this article in press as: Ammar A, et al., Closed loop torque SVM-DTC based on robust super twisting speed controller for induction motor drive with efficiency optimization, International Journal of Hydrogen Energy (2017), http://dx.doi.org/10.1016/j.ijhydene.2017.04.034

Loss minimization strategy LMC

The loss model control (LMC) strategy based on minimizing the motor losses in steady-state by adjusting the rotor and stator flux to an optimal value to achieve the maximum of efficiency and minimize the total losses especially at low load values. In our case a simplification will be proposed by neglecting the core losses in the optimization. The total copper losses expression is given by the sum of stator and rotor copper losses:

$$P_{c\_loss} = P_s + P_r \tag{15}$$

$$P_{c\_loss} = \frac{R_s}{M_{sr}^2}\psi_r^2 + \left[\frac{R_r}{p^2} + R_s\left(\frac{L_r}{pM_{sr}}\right)^2\right]\frac{T_e^2}{\psi_r^2} \tag{16}$$

The electromagnetic torque is given in field oriented d–q frame by:

$$T_e = p\frac{M_{sr}}{L_r}i_{sq} \tag{17}$$

The optimal flux can be founded in the steady state by setting the derivative of total copper loss expression with respect to the rotor flux to zero [21]:

$$\frac{\partial P_{c\_loss}}{\partial \psi_r} = 0 \tag{18}$$

Thus, the optimal reference value of the rotor flux $\psi^*_{r\_opt}$ is a function of the electromagnetic torque and the machine parameters in field oriented d–q system:

$$\psi^*_{r\_opt} = \lambda_{opt}\sqrt{T^*_e} \tag{19}$$

The coefficient λ_{opt} is given by:

$$\lambda_{opt} = \left(\frac{\lambda_2}{\lambda_1}\right)^{1/4} \tag{20}$$

where:

$$\lambda_1 = \frac{R_s}{M_{sr}^2};\quad \lambda_2 = \frac{R_r}{p^2} + R_s\left(\frac{L_r}{pM_{sr}}\right)^2$$

The imposed reference value of the rotor flux changes from a minimal to an optimal value according to the desired torque value [18,22]. For the DTC controlled induction motor drive, the optimal reference value of the stator flux $\psi^*_{s\_opt}$ can be deduced by the following expression [18]:

$$\psi^*_{s\_opt} = \frac{L_s}{M_{sr}}\sqrt{\left(\psi^*_{r\_opt}\right)^2 + \left(\frac{\sigma L_r}{p}\right)^2\left(\frac{T^*_e}{\psi^*_{r\_opt}}\right)} \tag{21}$$

Robust speed regulation

The common used controller in the outer speed loop to generate reference torque is the conventional PI controller. This paper presents a design of speed controller basing on the second order sliding mode control. The high order sliding mode is a generalized idea of the first order. It bases on higher order derivatives of the sliding surface. Besides keeping the same robustness and performance of sliding mode control, it reduces considerably the chattering phenomenon [10,23]. The nth sliding mode order can be determined by:

$$s = \dot{s} = \ddot{s} = \ldots = s^{(n-1)} = 0 \tag{22}$$

The super twisting is a second order sliding mode algorithm [13]. It can provide a continuous control by using only the information on s and evaluating the sign of $\dot{s}$ is not necessary. The convergence of this algorithm described by the rotation around the origin in the phase diagram$(s, \dot{s})$.

The super twisting (ST) control law $u(t)$ is formed of two parts. The first part is defined by its derivative with respect to time u_1 while the second is given by the function of the sliding variable u_2. The ST control law is defined by:

$$u_{ST} = u_1(t) + u_2(t) \tag{23}$$

where:

$$\begin{cases} u_2 = -\lambda|s|^{\rho}sign(s) + u_1 \\ \dot{u}_1 = -\beta sign(s) \end{cases} \tag{24}$$

λ and β are positive gains used to adjust the ST controller.

The degree of nonlinearity can be adjusted by the coefficient ρ which is defined by:

$$0 < \rho \leq 0.5 \tag{25}$$

Mostly it is fixed at "0.5" to realize the maximum of second order sliding mode control [24].

First order SM-speed controller design

The speed controller generates the reference torque T_{eref}. The sliding surface will be defined as:

$$\begin{cases} s_\omega = \omega_{ref} - \omega \\ \dot{s}_\omega = \dot{\omega}_{ref} - \dot{\omega} \end{cases} \tag{26}$$

The mechanical equation of induction motor is given as:

$$\dot{\omega} = \frac{1}{J}(T_e - T_L) - \frac{f}{J}\omega \tag{27}$$

J: inertia moment, f: coefficient of friction, T_L: Load torque.

By substituting Eq. (27) in the equation of the speed surface derivative, it will be given as follow:

$$\dot{s}_\omega = \dot{\omega}_{ref} - \frac{1}{J}(T_e - T_L - f\omega) \tag{28}$$

Basing on sliding mode theory, we can write:

$$T_e = T_{eeq} + T_{en} \tag{29}$$

The equivalent control part is defined during the sliding mode state $\dot{s}_\omega = 0$, then the equivalent control is:

$$T_{eeq} = \widehat{T}_L + f\omega \tag{30}$$

$\widehat{T}_L$ is the estimated load torque.

The discontinuous part is defined as:

$$T_{en} = Ksign(s_\omega) \tag{31}$$

K is a positive gain.

Please cite this article in press as: Ammar A, et al., Closed loop torque SVM-DTC based on robust super twisting speed controller for induction motor drive with efficiency optimization, International Journal of Hydrogen Energy (2017), http://dx.doi.org/10.1016/j.ijhydene.2017.04.034

Second order SM-speed controller design

In this section, the second order sliding mode speed control law will be designed by the combination of the defined equivalent control and the super twisting control law. The super twisting control law for speed controller (STSC) can be given as:

$$\begin{cases} u_{ST} = -\lambda_\omega |s_\omega|^{\frac{1}{2}} sign(s_\omega) + u_1 \\ \dot{u}_1 = -\beta_\omega sign(s_\omega) \end{cases} \quad (32)$$

λ_ω and β_ω are the super twisting speed controller gains. The control law convergence can be reached by an arbitrarily adjusting of these gains [24]. Generally, the gain λ_ω is more effective in system response. The gain β_ω has an effect in steady state accuracy. The sufficient conditions for a finite-time convergence are imposed by Levant in Ref. [23] as:

$$\begin{cases} \beta > \dfrac{\Phi}{\Gamma_M} \\ \lambda \geq \dfrac{4\Phi\Gamma_M(\beta+\Phi)}{\Gamma_m^3(\beta-\Phi)} \end{cases} \quad (33)$$

Φ is defined as the positive bounds of the uncertain function ϕ.

Γ_m and Γ_M are the lower and the upper positive bounds of the uncertain function γ at the second derivative of the sliding manifold (i.e. the rotor speed ω in our case) [23,24].

Where:

$$\Phi \geq \phi \text{ and } \Gamma_M \geq \gamma \geq \Gamma_m \quad (34)$$

$$\ddot{\omega} = \phi(x,t) + \gamma(x,t)\dot{u} \quad (35)$$

The controlled system can be simplified when it is linearly dependent on the control law u. Then, Φ, Γ_m and Γ_M will be considered as positives constants [9].

The generated reference torque by the second order sliding mode controller is given by:

$$T_{eref} = T_{eeq} + u_{ST} \quad (36)$$

The super twisting control law must fulfil Lyapunov stability condition to establish the speed control stability.

Stator flux estimation

The conventional back-emf integration approach of flux estimation can be expressed as:

$$\psi_s = \int_0^t (u_s - R_s i_s) dt \quad (37)$$

However, the implementation of an integrator for motor flux estimation is not an easy task. The pure integrator has DC-drift and initial value problems. The resulted flux estimation will include DC-flux component and the flux vector will not be estimated accurately. This leads also to DC-current component and severely affects motor operation. This DC components no matter how small, it can drive the integrator to saturation [25].

In this paper, a simple method used to remove the DC component from the estimated flux as shown in Fig. 4, where

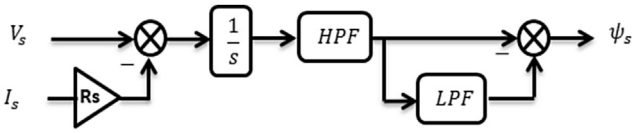

Fig. 4 – Modified flux estimator.

a high-pass filter (HPF) is used to extract the sinusoid. Since the HPF is not ideal and small DC offset could remain, another filtering is added where the remaining dc offset is extracted using a low pass filter (LPF) and subtracted from the output of the HPF. This approach was verified to eliminate all DC offset. The frequency should be low enough to avoid filtering the actual sinusoids when the machine operates at low speeds.

Fig. 5 shows the global block diagram of robust STSC based closed loop torque SVM-DTC with efficiency optimization.

Simulation and experimental results

Simulation results

The presented control algorithm has been simulated by Matlab/Simulink software. The simulation results were obtained for a three-phase 1.1 kW squirrel-cage induction motor with characteristics given in the Appendix. The simulation results show firstly the comparative study of the closed loop torque control (SVM-DTC) with constant flux reference (1 Wb) and optimal flux reference which generated by LMC strategy. In the second phase, the performance analysis of the optimized SVM-DTC control scheme with various speed controllers is presented.

Closed loop torque control SVM-DTC with constant and optimal flux references

The following figures (Figs. 6–11) illustrate the transient and the steady state with load introduction of 5 N m at t = 0.5s. The figures are specified by (a) for the constant and (b) for optimal flux reference. The Fig. 12 shows the total losses and the efficiency for both cases.

Firstly, Figs. 6–8 present flux magnitude, components and circular trajectory, we can see that it has low ripples level due to the use of the SVM modulation. Furthermore, the proposed strategy with LMC show the optimal flux variation in Figs. 6(b)–8(b) according to the load application contrary to the constant flux value in Fig. 6(a)–8(a). After the transient state, it can be observed that the flux takes and optimal value in the steady state in order to minimize the losses, consequently, the optimized technique shows its performance. Fig. 9 shows the evolution of flux trajectory in 3D presentation, this figure can explain clearly the optimal flux variation and conclude the main idea of this optimization. Next, in Fig. 10, the electromagnetic torque is shown. Due to the effect of SVM, the torque response shows low ripples in both cases, Moreover, the optimized algorithm presents a reducer ripples level especially at no load state. Fig. 11 illustrates the stator phase current, we can notice in Fig. 7 (b) that the proposed technique shows an apparent reduction in current amplitude at no low load operation owing to the optimal flux choice. This

Please cite this article in press as: Ammar A, et al., Closed loop torque SVM-DTC based on robust super twisting speed controller for induction motor drive with efficiency optimization, International Journal of Hydrogen Energy (2017), http://dx.doi.org/10.1016/j.ijhydene.2017.04.034

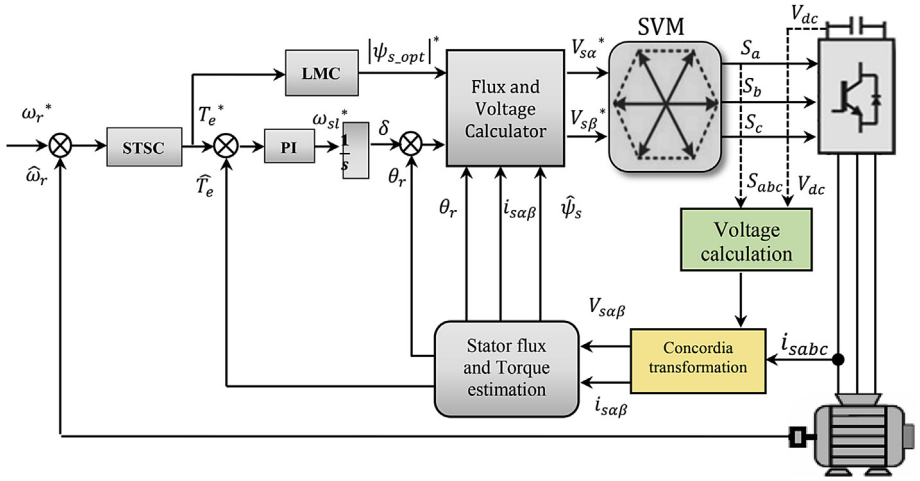

Fig. 5 – Robust closed loop torque SVM-DTC with super twisting speed controller and LMC strategy.

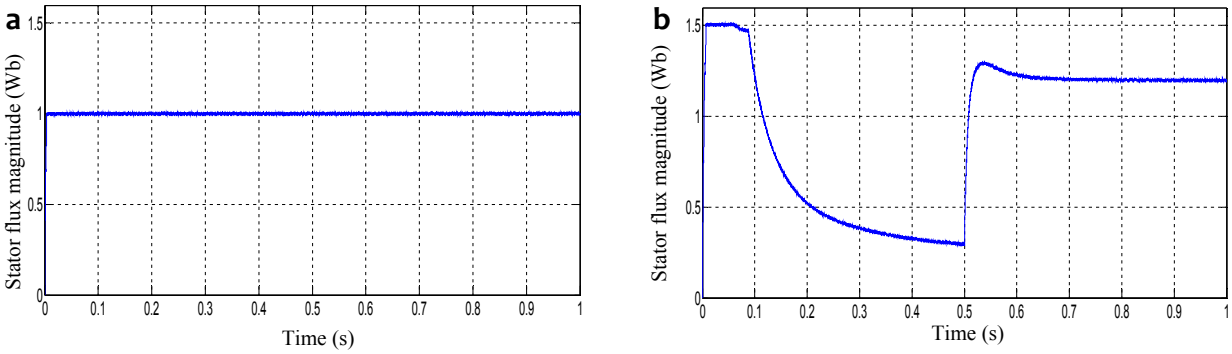

Fig. 6 – Stator flux magnitude (Wb).

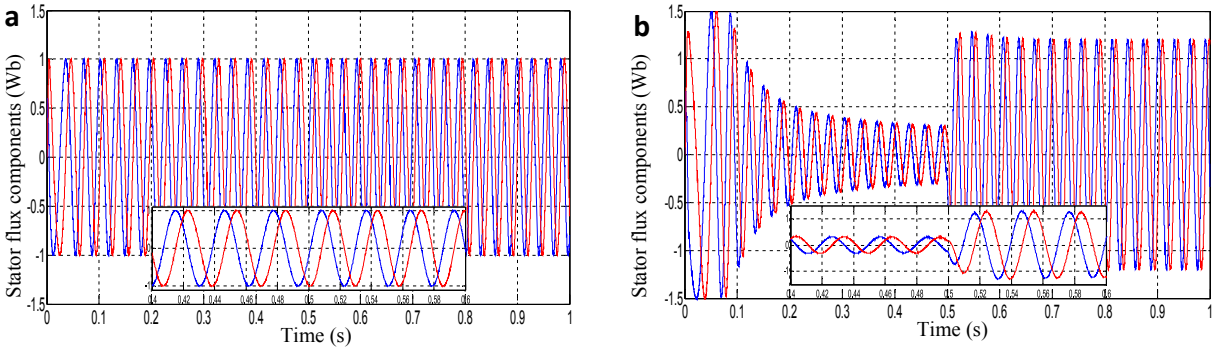

Fig. 7 – Stator flux components (α, β) (Wb).

reduction can reduce considerably the copper losses in this state. Then, the Fig. 12 shows the total losses and efficiency of both control algorithm, we deduce that the optimized SVM-DTC with LMC has the lower losses value at no load or at light load state, as a result, it provides the better efficiency than using fixed flux reference.

PI and STSC speed controllers comparative analysis

In this section, the second order super twisting controller is compared to a classical PI controller for the speed regulation in outer loop of the optimized control strategy. The figures are specified by (a) for PI and (b) for super twitting controller.

Figs. 13 and 14(a–b) illustrate the rotor speed and the electromagnetic torque of the control algorithm associated with PI and super twisting controllers while speed sense reversing (1000; −1000 rpm). The super twisting controller in Figs. 13 and 14(b) presents better speed and torque responses during the starting up and the sense reversing compared to the conventional PI in Figs. 13 and 14(a). Furthermore, the

Please cite this article in press as: Ammar A, et al., Closed loop torque SVM-DTC based on robust super twisting speed controller for induction motor drive with efficiency optimization, International Journal of Hydrogen Energy (2017), http://dx.doi.org/10.1016/j.ijhydene.2017.04.034

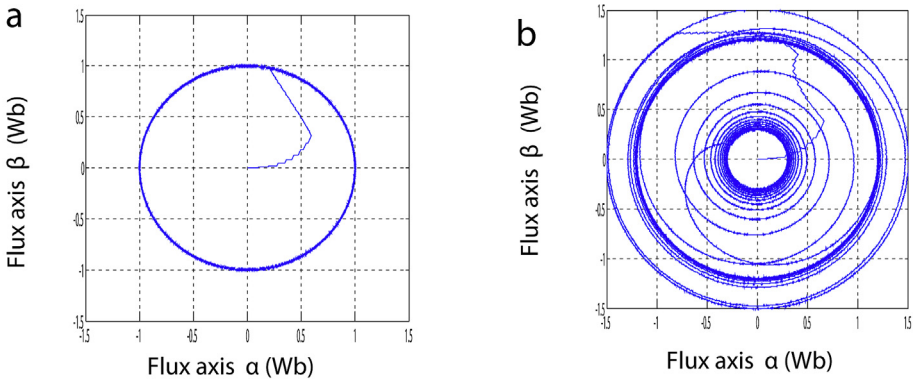

Fig. 8 – Stator flux trajectory (Wb).

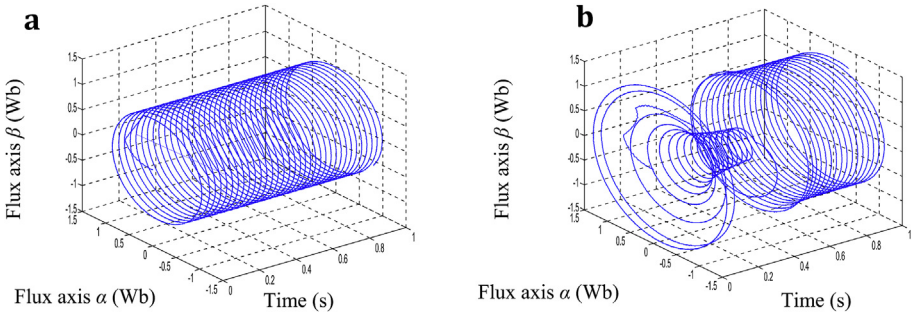

Fig. 9 – Stator flux trajectory in 3D presentation (Wb).

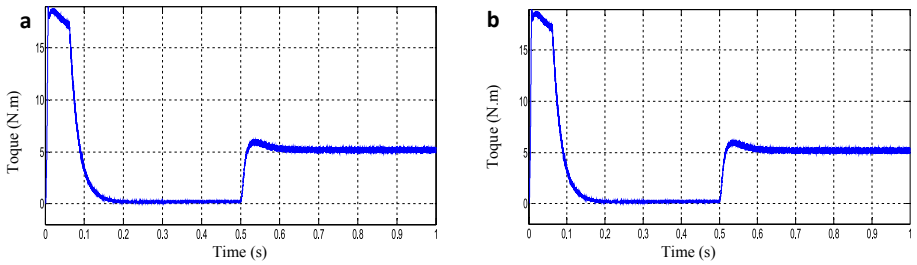

Fig. 10 – Electromagnetic torque with load application of (5 N m).

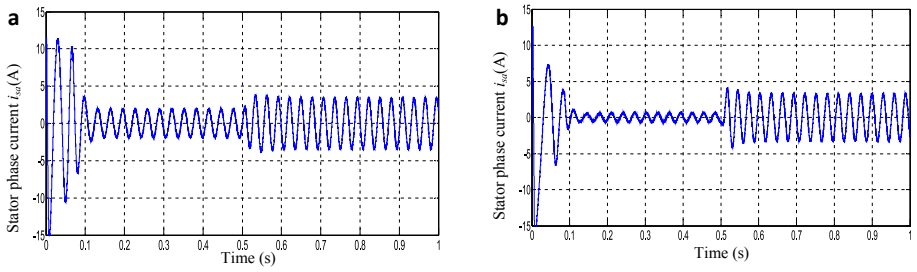

Fig. 11 – Stator phase current i_{sa} (A).

comparison shows that the influence by the load application of the SVM-DTC with STSC is not considerable and the torque has faster responding as illustrated in (Figs. 13 and 14(b) ZOOM). We can also notice that the super twisting controller is featured by the reduced chattering level, this problem has been eliminated by applying the second order control law. The next Table 1 presents a summarized comparative analysis of both of speed controllers.

Please cite this article in press as: Ammar A, et al., Closed loop torque SVM-DTC based on robust super twisting speed controller for induction motor drive with efficiency optimization, International Journal of Hydrogen Energy (2017), http://dx.doi.org/10.1016/j.ijhydene.2017.04.034

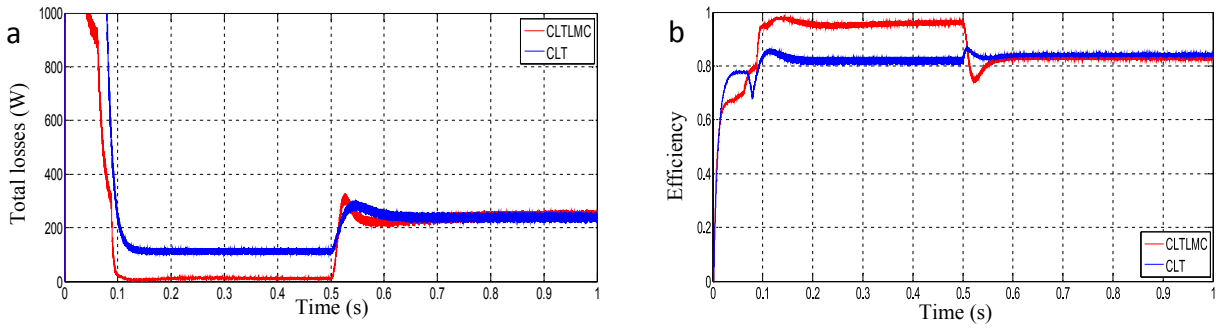

Fig. 12 – Total losses and efficiency.

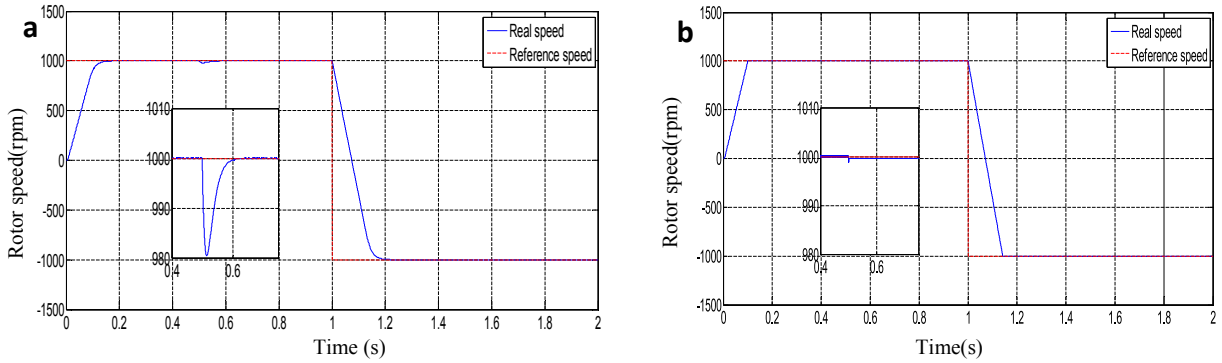

Fig. 13 – Rotor Speed during rotation sense reversing (1000 rpm;−1000 rpm) for PI and STSC controllers.

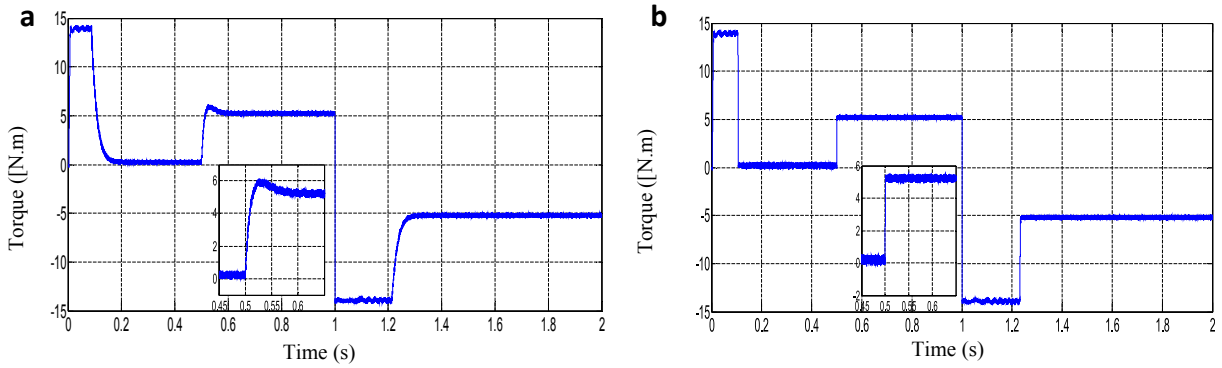

Fig. 14 – Torque response during rotation sense reversing (1000 rpm;−1000 rpm) for PI and STSC controllers.

Table 1 – Comparative analysis of the various controllers in outer speed loop (PI, STSC).

	PI	STSC
Speed response time [sec]	0.12 s	0.095 s
Speed dropping due to load application [rpm, %]	28 rpm 2.8%	1.2 rpm 0.12%
Torque response time to load application [sec]	0.026 s	0.006 s

Experimental results

The real-time control of the robust optimized SVM-DTC was done in the laboratory equipped by dSpace 1104 board. The implementation ground of induction motor real time control is shown in Fig. 15. It is composed of 1: A squirrel-cage IM 1.1 kW. 2: Semikron power converter composed of a rectifier and IGBT inverter. 3: incremental encoder (position and speed sensor). 4: dSpace DS 1104 with 5: control desk software plugged in personnel computer. 6: Magnetic powders break with load control unit. 7: Hall type current sensors. 8: voltage sensors. 9: GW-INSTEK numerical oscilloscope will be used for results extraction. To reduce the cost of the control system, the phase voltages will be estimated from DC-bus and inverter switching states (S_a, S_b, S_c) [7]. The following figures show the conducted experimental tests which are the same as the presented tests in the simulation section. The experimental results are specified also by (a) for the constant and (b) for optimal flux reference. In addition, by (a) for PI and (b) for STSC speed controllers in Figs. 20 and 21.

Please cite this article in press as: Ammar A, et al., Closed loop torque SVM-DTC based on robust super twisting speed controller for induction motor drive with efficiency optimization, International Journal of Hydrogen Energy (2017), http://dx.doi.org/10.1016/j.ijhydene.2017.04.034

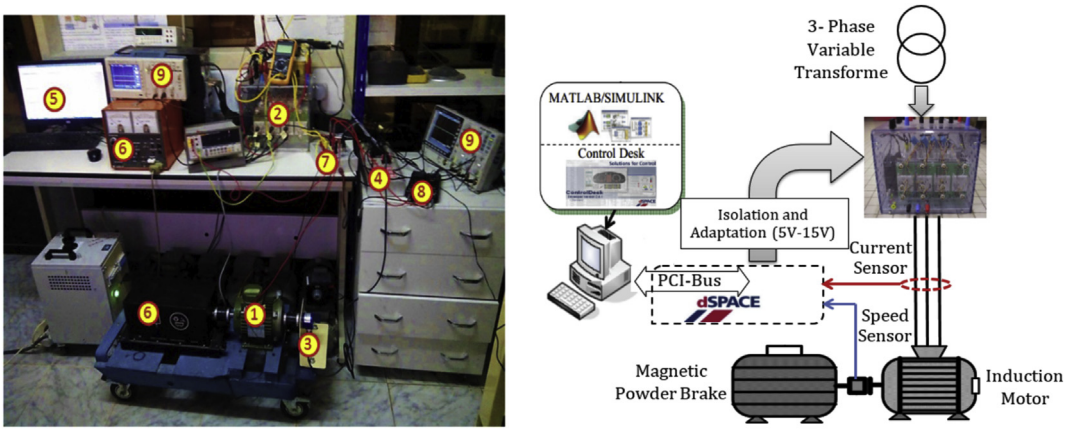

Fig. 15 – Experimental setup.

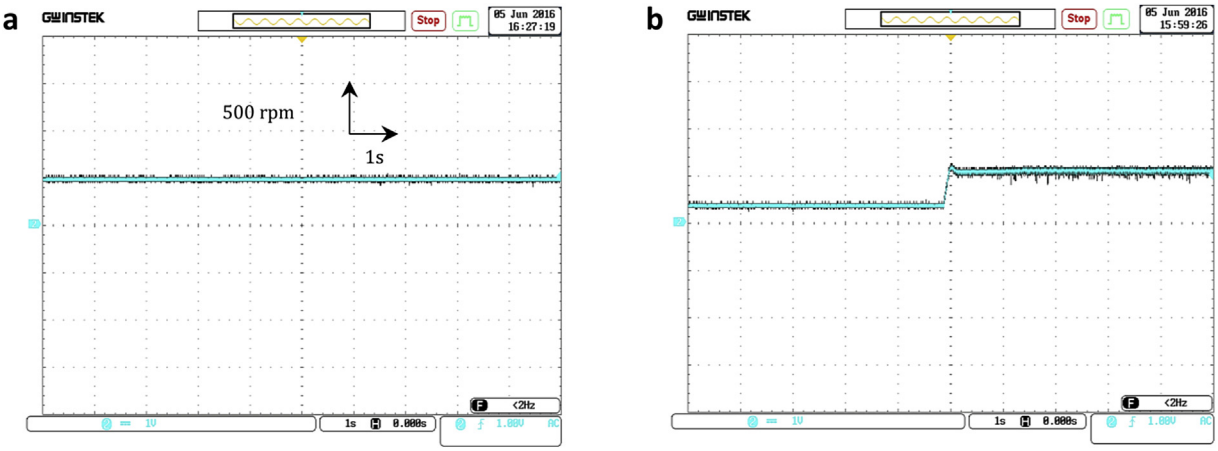

Fig. 16 – Stator flux magnitude (Wb).

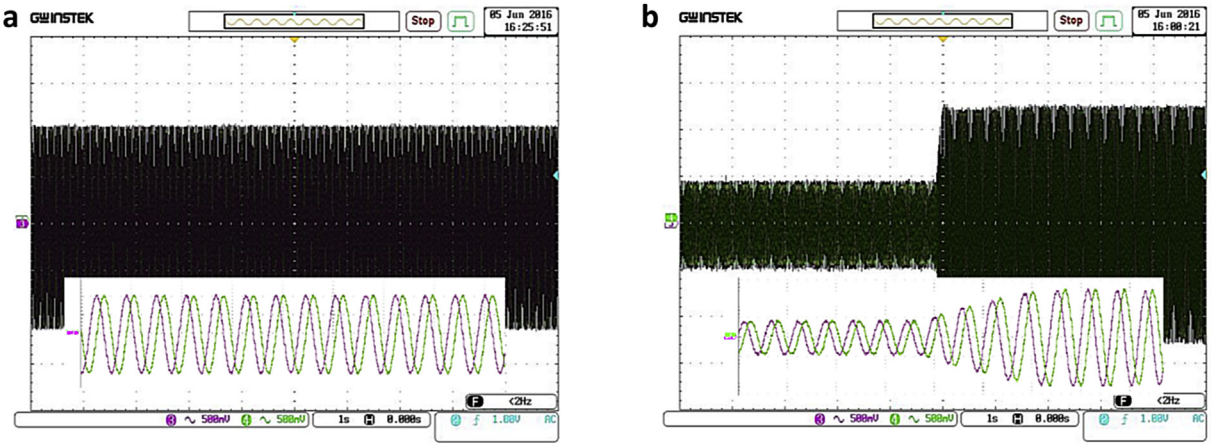

Fig. 17 – Stator flux components with zoom (Wb).

The experimental results have been obtained by using GW-INSTEK numerical oscilloscope which linked with the real-time interface. The accomplished tests are the same as the simulation results. Figs. 16–18 show the comparison between the constant and optimal flux reference variation according to the load application, the obtained result are similar to those obtained by simulation. Fig. 19 illustrates the electromagnetic torque ($1div = 5N\ m$) and stator phase current with load introduction. The torque shows low ripples and good response to the load application and stator phase current presents a good waveform. The optimized technique has the reducer ripples level and the lower current amplitude at no load state

Please cite this article in press as: Ammar A, et al., Closed loop torque SVM-DTC based on robust super twisting speed controller for induction motor drive with efficiency optimization, International Journal of Hydrogen Energy (2017), http://dx.doi.org/10.1016/j.ijhydene.2017.04.034

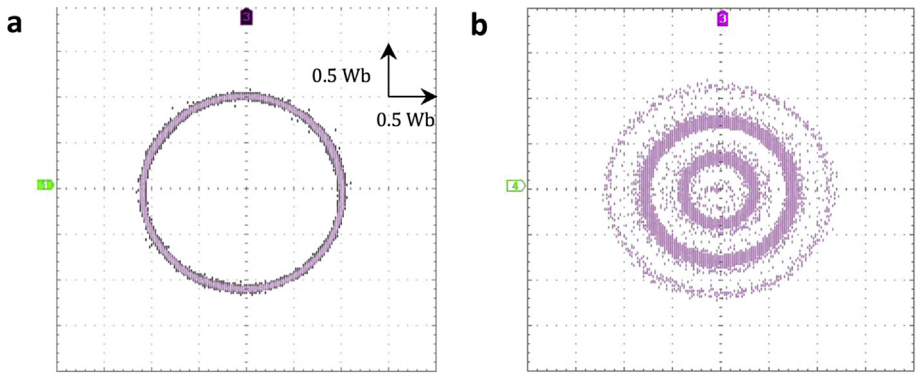

Fig. 18 – Stator flux trajectory (Wb).

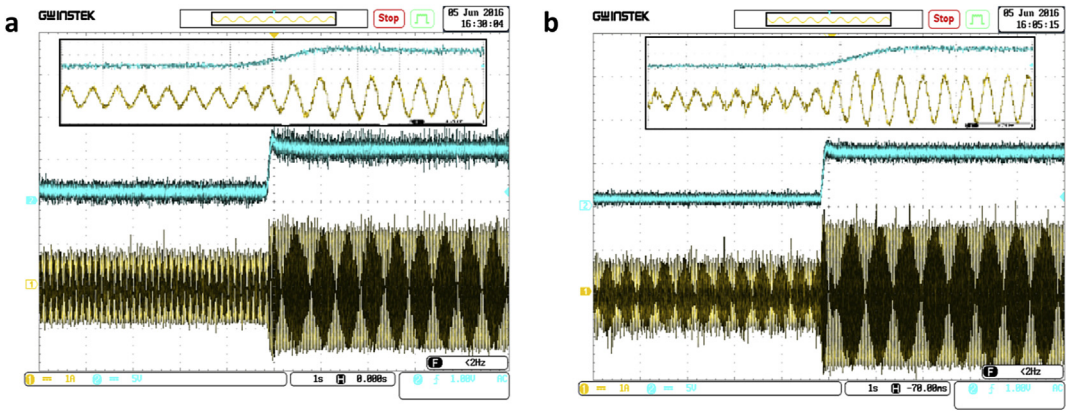

Fig. 19 – Electromagnetic torque (N m) and stator phase currents (A).

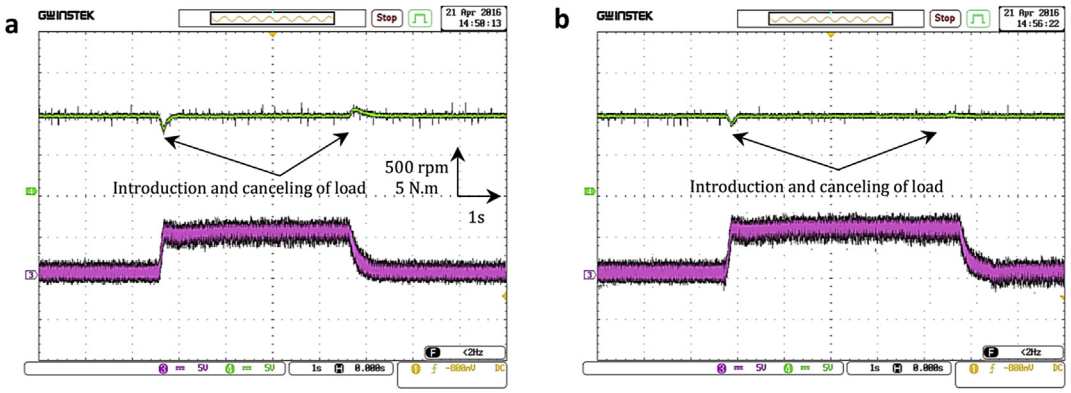

Fig. 20 – Rotor speed (rpm) and torque responses (N m) for PI and STSC controllers.

due to the supposed optimal flux reference, this latter can minimize the losses and improve the efficiency in this operation mode.

Secondly, the comparison of ST (super twisting) and PI controllers for speed regulation loop is shown in Figs. 20 and 21. Fig. 20 presents the speed response and electromagnetic torque while the introduction and the cancelling of the load for both ST and PI controllers, the figure shows that the STSC is more robust against external load disturbance compared with PI controller. After that, Fig. 21 presents the rotor speed reversing response, the ST shows a perfect superposition and provides a better tracking than PI and it reduces the overshoot.

In general, the experimental results have validated the simulation by giving a similar behaviour in all tests. However, it is noticed that there is a small disagreement between the results. This is owing to many reasons. The limited sampling time of the processor, the inaccuracies and different constraints which exist in the real-time implementation, the dead times of the inverter switching signals and measurement instrumentations offset.

Please cite this article in press as: Ammar A, et al., Closed loop torque SVM-DTC based on robust super twisting speed controller for induction motor drive with efficiency optimization, International Journal of Hydrogen Energy (2017), http://dx.doi.org/10.1016/j.ijhydene.2017.04.034

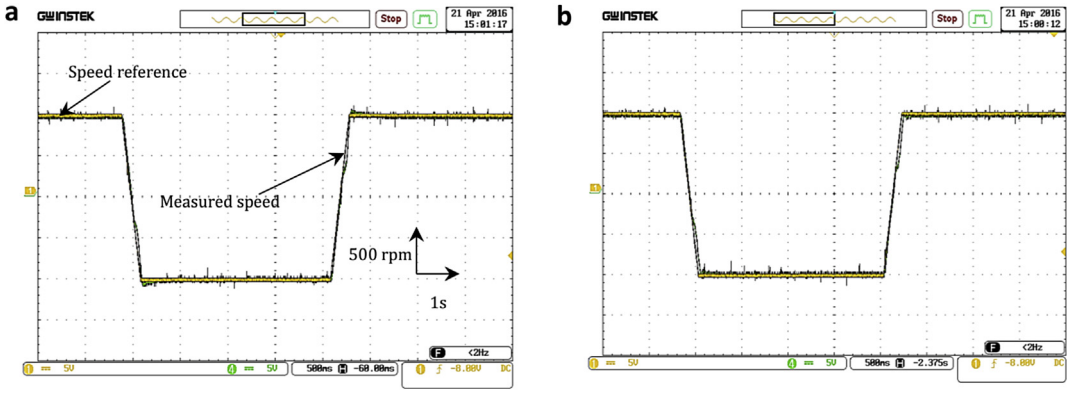

Fig. 21 – Rotor Speed during rotation sense reversing for PI and STSC controllers.

Conclusion

In this paper, we present a simulation and real-time implementation of an optimized closed loop torque SVM-DTC strategy with model based losses minimization strategy (LMC) and robust speed controller based on super twisting strategy. The proposed control technique has been presented in order to improve performance of the classical DTC and to optimize the IM energy as a second objective.

The proposed strategy using SVM has many advantages those are verified by simulation and experimentally using dSpace platform, such as reduced torque and flux ripples, good waveforms of stator current and constant switching frequency. The application of robust super twisting controller instead of conventional PI gives more high performances for the control scheme like the robustness against disturbance and fast response. In the other hand, the effectiveness and performances of LMC which based on the choosing of an optimal flux reference have been also verified and compared with the basic technique which uses a constant flux reference. The simulation and experimental validation gives similar results, they show that LMC reduces losses and improves efficiency at zero and low loads operation. Therefore, DTC-SVM is a good solution in general to overcome the drawbacks of classical DTC. The coupling with LMC and robust algorithms can get higher performance and efficiency for induction motor drive control.

Appendix

The parameters of the three-phase Induction motor, employed for real time implementation, in SI units are: 1.1 kW, 50 Hz, p = 2, R_s = 6.75Ω, R_r = 6.21Ω, R_f = 1800 Ω, $L_s = L_r = 0.5192$ H, $M_{sr} = 0.4957$ H, $f = 0.002$ SI, $J = 0.01240$ kg m^2.

REFERENCES

[1] Alsofyani IM, Idris NRN. Simple flux regulation for improving state estimation at very low and zero speed of a speed sensorless direct torque control of an induction motor. IEEE Trans Power Electron 2016;31:3027–35. http://dx.doi.org/10.1109/TPEL.2015.2447731.

[2] Lascu C, Boldea I, Blaabjerg F. A modified direct torque control for induction motor sensorless drive. IEEE Trans Ind Appl 2000;36:122–30. http://dx.doi.org/10.1109/28.821806.

[3] Naik V, Panda A, Singh SP. A three-level Fuzzy-2 DTC of induction motor drive using SVPWM. IEEE Trans Ind Electron 2016;63:1467–79. http://dx.doi.org/10.1109/TIE.2015.2504551.

[4] Habibullah M, Lu DD, Xiao D, Rahman MF. A simplified finite-state predictive direct torque control for induction motor drive. IEEE Trans Ind Electron 2016;63:3964–75. http://dx.doi.org/10.1109/TIE.2016.2519327.

[5] Rodriguez J, Pontt J, Silva C, Kouro S, Miranda H. A novel direct torque control scheme for induction machines with space vector modulation. In: IEEE 35th Annu Power Electron Spec Conf (IEEE Cat No04CH37551); 2004. p. 1392–7. http://dx.doi.org/10.1109/PESC.2004.1355626.

[6] Ammar A, Bourek A, Benakcha A. Sensorless SVM-direct torque control for induction motor drive using sliding mode observers. J Control Autom Electr Syst 2017;28:189–202. http://dx.doi.org/10.1007/s40313-016-0294-7.

[7] Ammar A, Bourek A, Benakcha A. Modified load angle Direct Torque Control for sensorless induction motor using sliding mode flux observer. In: 2015 4th Int Conf Electr Eng IEEE; 2015. p. 1–6. http://dx.doi.org/10.1109/INTEE.2015.7416602.

[8] Lekhchine S, Bahi T, Abadlia I, Bouzeria H. PV-battery energy storage system operating of asynchronous motor driven by using fuzzy sliding mode control. Int J Hydrogen Energy 2016:1–9. http://dx.doi.org/10.1016/j.ijhydene.2016.05.298.

[9] Ammar A, Bourek A, Benakcha A. Nonlinear SVM-DTC for induction motor drive using input-output feedback linearization and high order sliding mode control. ISA Trans 2017;67:428–42. http://dx.doi.org/10.1016/j.isatra.2017.01.010.

[10] Di Gennaro S, Rivera Dominguez J, Meza MA. Sensorless high order sliding mode control of induction motors with core loss. IEEE Trans Ind Electron 2014;61:2678–89. http://dx.doi.org/10.1109/TIE.2013.2276311.

[11] Matraji I, Laghrouche S, Wack M. Pressure control in a PEM fuel cell via second order sliding mode. Int J Hydrogen Energy 2012;37:16104–16. http://dx.doi.org/10.1016/j.ijhydene.2012.08.007.

[12] Evangelista C, Puleston P, Valenciaga F. Wind turbine efficiency optimization. Comparative study of controllers based on second order sliding modes. Int J Hydrogen Energy 2010;35:5934–9. http://dx.doi.org/10.1016/j.ijhydene.2009.12.104.

[13] Matraji I, Ahmed FS, Laghrouche S, Wack M. Comparison of robust and adaptive second order sliding mode control in PEMFC air-feed systems. Int J Hydrogen Energy 2015;40:9491–504. http://dx.doi.org/10.1016/j.ijhydene.2015.05.090.

Please cite this article in press as: Ammar A, et al., Closed loop torque SVM-DTC based on robust super twisting speed controller for induction motor drive with efficiency optimization, International Journal of Hydrogen Energy (2017), http://dx.doi.org/10.1016/j.ijhydene.2017.04.034

[14] Derbeli M, Farhat M, Barambones O. Control of PEM fuel cell power system using sliding mode and super-twisting algorithms. Int J Hydrogen Energy 2016:1–12. http://dx.doi.org/10.1016/j.ijhydene.2016.06.103.
[15] Haddoun A, El M, Benbouzid H, Member S, Diallo D, Member S, et al. A Loss-Minimization DTC Scheme for EV Induction Motors 2007; 56: 81–88. 10.1109/TVT.2006.889562.
[16] Abrahamsen F, Blaabjerg F, Member S, Pedersen JK, Grabowski PZ, Member S, et al. On the energy optimized control of standard and high-efficiency induction motors in ct and hvac applications 1998; 34: 822–831.
[17] Uddin MN, Member S, Nam SW. New online loss-minimization-based control of an induction motor drive 2008; 23: 926–933.
[18] Tazerart F, Mokrani Z, Rekioua D, Rekioua T. Direct torque control implementation with losses minimization of induction motor for electric vehicle applications with high operating life of the battery. Int J Hydrogen Energy 2015;40:13827–38. http://dx.doi.org/10.1016/j.ijhydene.2015.04.052.
[19] Kumsuwan Y, Premrudeepreechacharn S, Toliyat HA. Modified direct torque control method for induction motor drives based on amplitude and angle control of stator flux. Electr Power Syst Res 2008;78:1712–8. http://dx.doi.org/10.1016/j.epsr.2008.02.015.
[20] Uddin M, Hafeez M. FLC-based DTC scheme to improve the dynamic performance of an IM drive. IEEE Trans Ind Appl 2012;48:823–31. http://dx.doi.org/10.1109/TIA.2011.2181287.
[21] Kennel R. Loss minimization of induction machines in dynamic operation. IEEE Trans Energy Convers 2013:1–10. http://dx.doi.org/10.1109/TEC.2013.2262048.
[22] Rehman H, Xu L. Alternative energy vehicles drive system: control, flux and torque estimation, and efficiency optimization 2011; 60: 3625–3634.
[23] Levant A. Higher-order sliding modes, differentiation and output-feedback control. Int J Control 2003;76:924–41. http://dx.doi.org/10.1080/0020717031000099029.
[24] Rashed M, Goh KB, Dunnigan MW, MacConnell PFA, Stronach AF, Williams BW. Sensorless second-order sliding-mode speed control of a voltage-fed induction-motor drive using nonlinear state feedback. IEE Proc Electr Power Appl 2005;152:1127. http://dx.doi.org/10.1049/ip-epa:20050042.
[25] Singh B, Jain S, Dwivedi S. Torque ripple reduction technique with improved flux response for a direct torque control induction motor drive. IET Power Electron 2013;6:326–42. http://dx.doi.org/10.1049/iet-pel.2012.0121.

Please cite this article in press as: Ammar A, et al., Closed loop torque SVM-DTC based on robust super twisting speed controller for induction motor drive with efficiency optimization, International Journal of Hydrogen Energy (2017), http://dx.doi.org/10.1016/j.ijhydene.2017.04.034